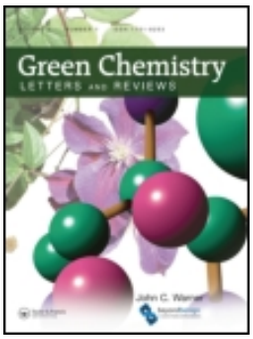

Green Chemistry Letters and Reviews

ISSN: 1751-8253 (Print) 1751-7192 (Online) Journal homepage: informahealthcare.com/journals/tgcl20

Green synthesis of silver chloride nanoparticles using *Prunus persica* L. outer peel extract and investigation of antibacterial, anticandidal, antioxidant potential

Jayanta Kumar Patra & Kwang-Hyun Baek

To cite this article: Jayanta Kumar Patra & Kwang-Hyun Baek (2016) Green synthesis of silver chloride nanoparticles using *Prunus persica* L. outer peel extract and investigation of antibacterial, anticandidal, antioxidant potential, Green Chemistry Letters and Reviews, 9:2, 132-142, DOI: 10.1080/17518253.2016.1192692

To link to this article: https://doi.org/10.1080/17518253.2016.1192692

Published online: 13 Jun 2016.

GREEN CHEMISTRY LETTERS AND REVIEWS, 2016
VOL. 9, NO. 2, 132–142
http://dx.doi.org/10.1080/17518253.2016.1192692

Taylor & Francis
Taylor & Francis Group

OPEN ACCESS

Green synthesis of silver chloride nanoparticles using *Prunus persica* L. outer peel extract and investigation of antibacterial, anticandidal, antioxidant potential

Jayanta Kumar Patra[a] and Kwang-Hyun Baek[b]

[a]Research Institute of Biotechnology & Medical Converged Science, Dongguk University, Ilsandong-gu, Gyeonggi-do, Republic of Korea; [b]Department of Biotechnology, Yeungnam University, Gyeongsan, Gyeongbuk, Republic of Korea

ABSTRACT

The present study was conducted to synthesize silver chloride nanoparticles using the aqueous extract of outer peel of peach fruit (*Prunus persica* L.) and to evaluate its antibacterial activity, synergistic antibacterial and anticandidal potential against five foodborne pathogenic bacteria and five pathogenic *Candida* species respectively along with its antioxidant potential. The synthesized silver chloride nanoparticles (PE-AgClNPs) were visually confirmed with surface plasmon resonance peak at 440 nm upon UV–Vis spectroscopy analysis. Furthermore, the morphology, elemental composition and crystallinity nature were also characterized. PE-AgClNPs displayed strong antibacterial potentials (9.01–10.83 mm inhibition zone) against foodborne pathogenic bacteria and increased synergistic effect with kanamycin and rifampicin. PE-AgClNPs also displayed strong anticandidal synergistic activity with standard amphotericin b (10.51–14.01 mm inhibition zones), along with strong free radical scavenging and reducing power. Based on strong antibacterial and antioxidant capacities, PE-AgClNPs are anticipated to have potential applications in the biomedical and food sector industries.

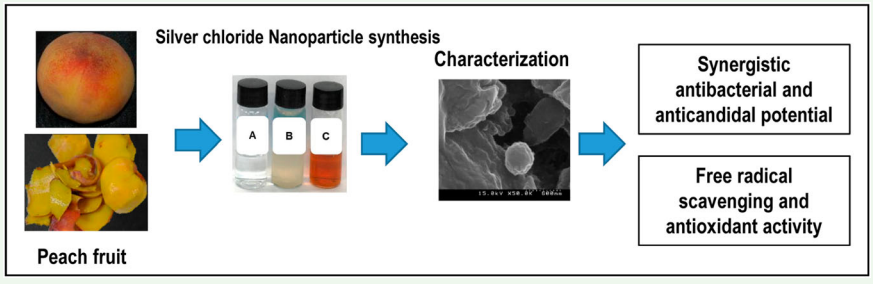

ARTICLE HISTORY
Received 11 February 2016
Accepted 18 May 2016

KEYWORDS
FT-IR spectroscopy; peach peel; silver nanoparticles; synergistic effect; XRD spectroscopy

1. Introduction

Silver nanoparticles (Ag nanoparticles) are gaining interest among the scientific community because of their distinct properties, which include good chemical stability, catalytic properties, electrical conductivity and antibacterial potential (*1*). Ag nanoparticles have a number of applications, especially as antimicrobial agents with potential for use in the cosmetics, medical, electronics and textile industries (*2*). The antibacterial potential of Ag nanoparticles has made them a potential candidate for use in the formulation of dental resin composites and ion exchange fibers, as well as in coatings for various surgical medical devices (*3*, *4*). Furthermore, they have been used in the food industry as a component of food packaging materials that can easily block the entry of moisture, CO_2 and O_2 from reaching fresh fruits, vegetables, meats and other processed food products (*5*). Excess generation of free radicals in the body plays an important role in many degenerative diseases such as aging, cancer and cardiovascular conditions (*6*). Moreover, a number of inorganic nanoparticles have been found to be effective against the adverse effects of free radicals (*7*).

There has been a great deal of effort made for the biosynthesis of metal nanoparticles including Ag using biological sources such as microorganisms, plants and plant products, which are environmental benign and eco-friendly (*8–11*). Different plants and their products have been reported to be utilized in biological processes for the synthesis of nanoparticles (*6*, *12–16*). The outer peels of fruits contain various beneficial natural compounds;

CONTACT Kwang-Hyun Baek khbaek@ynu.ac.kr

however, they are usually discarded as waste. Therefore, utilization of the outer peels for the synthesis of nanoparticles can be the first step toward the use of waste materials in the synthesis of nanoparticles.

Peach (*Prunus persica* L.) is a climacteric fruit that originated from the Asian continent mainly China (*17*). It is cultivated in many countries, but preferably in temperate regions, as it requires abundant water (*18*). It contains high quantity of water, sugar and protein along with vitamins and minerals (*19*). It also contains phenolic compounds such as catequins and leucoanthocyanins (*19*). The major phenolic compounds identified in peach are chlorogenic acid, catechins and epicatechins, with other compounds, including gallic acid, ellagic acid, rutin and isoquercetin (primary flavonols), cyanidin glucosides (anthocyanins) and malvin glycosides (*20–23*). The presence of carotenoids such as β-cryptoxantine, β-carotene and α-carotene has been detected in peach fruit together with zeaxanthine, lycopene and xanthophyll. Peaches are rich in carbohydrates, group B vitamins, including vitamin C (or L-ascorbic acid) and niacin (vitamin B3). Ripen juicy pulp of the fruit is edible, whereas the peel is discarded. Earlier literature has clearly presented that the outer peel of the fruit contained higher amounts of phenolics than the pulp, and anthocyanins and flavonols were primarily detected in the peel (*19*). Apart from these, the different peach cultivars are rich in hydroxycinnamates and flavan-3-ols with relatively higher antioxidant activities (*19, 24–26*).

In this context, the present study was conducted to investigate the synthesis of Ag nanoparticles using the outer peel extract of peach fruits (*P. persica* L.), which are produced in large amounts by the canned peach industry but mainly treated as waste. In addition to synthesis of Ag nanoparticles using outer peels, we also evaluated their antibacterial activity against foodborne bacteria, anticandidal activity against pathogenic *Candida* species and antioxidant potentials.

2. Experimental

2.1. Chemicals and pathogenic bacteria

All chemicals, including 2,2′-azino-bis[3-ethylbenzothiazoline-6-sulfonic acid] (ABTS), ascorbic acid, 1,1-diphenyl-2-picrylhydraxyl (DPPH), Griess reagent and Ag nitrate ($AgNO_3$), were purchased from Sigma-Aldrich (St. Louis, MO, USA). Nutrient agar (NA) and nutrient broth were purchased from Becton, Dickinson and Company (Franklin Lakes, New Jersey, USA). Foodborne pathogenic bacteria, namely *Bacillus cereus* ATCC 13061, *Listeria monocytogenes* ATCC 19115, *Staphylococcus aureus* ATCC 49444, *Escherichia coli* ATCC 43890 and *Salmonella Typhimurium* ATCC 43174), were obtained from the American Type Culture Collection (ATCC, Manassas, VA, USA). Fully ripened peaches were obtained from a local market at Gyeongsan (Gyeongbuk, Republic of Korea).

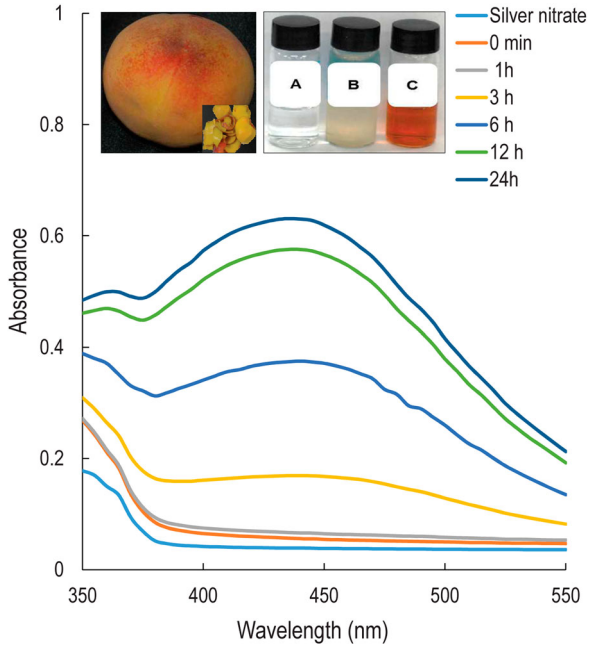

Figure 1. UV–Vis spectra of silver nanoparticles (PE-AgClNPs) synthesized by the peach outer peel extracts (PE). Inset: fruit and outer peel of peach (*P. persica L.*) (left); Change in color of the solution confirming the synthesis of PE-AgClNPs ((a) – $AgNO_3$ solution, (b) – peach outer peel extracts (PE), (c) – PE-AgClNPs) (Right).

2.2. Preparation of extract from peach outer peel

Five fresh, fully ripened peaches were washed manually two times in running tap water, then one time in double distilled water. The outer peels of the peaches (Figure 1, inset) were subsequently cut into small pieces (about 10–15 mm size) and weighed. Next, 20 g of the outer peel was placed in 100 mL of deionized water in a 250 mL conical flask and boiled for 10 min with continuous stirring using a magnetic stirrer. The peach aqueous extract (PE) was then cooled to room temperature, filtered through Whatman No. 1 filter paper and stored in a sterilized bottle at 4°C until further use.

2.3. Synthesis of Ag nanoparticles using PE

Ag nanoparticles were synthesized by the reduction of $AgNO_3$ solution by PE extract. Briefly, 10 mL of PE extract was slowly added to 100 mL of 1 mM $AgNO_3$ in a 250 mL conical flask with continuous stirring at room temperature. The reduction of $AgNO_3$ to Ag-nanoparticles by PE (PE-AgNP) was monitored visually by the change in color of the solution from colorless to

reddish brown. Following synthesis, the solution with PE-AgNP was centrifuged at 10,000 rpm for 30 min using a high-speed centrifuge (Supra 22 K, Hanil Science Industrial, Republic of Korea). The pellet was then acquired, washed twice in distilled water and dried to powder using a vacuum dryer (LVS 201T, Ilmvac GmbH, Germany, UK).

2.4. Characterization of PE-AgClNPs

The synthesized PE-AgClNPs were characterized by various analytical measurements including UV–Vis spectroscopy, scanning electron microscopy (SEM), energy-dispersive X-ray (EDX) analysis, X-ray powder diffraction (XRD) analysis, thermo-gravimetric analysis (TGA) and Fourier transform infrared spectroscopy (FT-IR), as previously described (*4*, *6*, *10*, *13*, *14*).

2.4.1. UV–Vis spectroscopy

Briefly, the reduction of Ag^+ ions to Ag-nanoparticles was monitored by measuring the absorption spectra of the solution at a resolution of 1 nm between 350 nm and 550 nm at different time intervals up to 48 h using a microplate reader (Infinite 200 PRO NanoQuant, TECAN, Switzerland).

2.4.2. SEM and EDX analysis

For morphological characteristics, the PE-AgClNPs were uniformly spread and sputter coated with platinum using an ion coater for 120 s, then observed under a SEM (S-4200, Hitachi, Japan). The particle size of the synthesized nanoparticles was calculated from the enlarged SEM image. The elemental composition of the powdered PE-AgClNPs was subsequently analyzed using an EDX detector (EDS, EDAX Inc., Mahwah, New Jersey, USA) attached to the SEM machine.

2.4.3. X-ray diffraction analysis

The Franklin Lakes, structures of the synthesized PE-AgClNPs, were determined with an XRD machine (X'Pert MRD, PANalytical, Almelo, The Netherlands) at a machine setup of 30 kV, 40 mA, with Cu Kα radians at an angle of 2θ. The particle size of PE-AgClNPs was determined from the Scherer equation (*27*).

2.4.4. TGA analysis

The TGA analysis of the powdered PE-AgClNPs was measured with a TGA machine (SDT Q600, TA Instruments, New Castle, DE, USA) using an alumina pan in a temperature range of 20–700°C while ramping at 10°C/min. Prior to analysis about 5 mg of the powdered PE-AgClNPs was weighed in a clean dry alumina pan and placed under the TGA machine and analyzed for the degradation of organic matter with increase in temperature.

2.4.5. FT-IR analysis

The FT-IR spectra of the powdered PE-AgClNPs was acquired by a FT-IR spectrophotometer (Jasco 5300, JASCO, Mary's Court, Easton, MD, USA) at wavelengths ranging from 400 cm^{-1} to 4000 cm^{-1}. For the FTIR analysis, the powdered sample was ground with KBr at a 1:100 ratio and a thin film of the sample was prepared using the specially designed screw knot and analyzed for the presence of different types of functional groups responsible for synthesis of PE-AgClNPs from the different mode of vibrations.

2.5. Antimicrobial potential of PE-AgClNPs

2.5.1. Determination of antibacterial activity of PE-AgClNPs

The antibacterial potential of PE-AgClNPs was determined against five different foodborne bacteria by the standard disc diffusion method (*28*). Prior to use, powders of the PE-AgClNPs were dissolved at 1000 µg/mL in 5% dimethylsulfoxide (DMSO), after which a colloidal solution was prepared by sonication for 15 min at 30°C. Each filter paper disc with 50 µg PE-AgClNPs was prepared for the assay and 5% DMSO was taken as the negative control. The filter paper discs were placed on overnight cultures of the foodborne bacteria grown on NA plates and then incubated for an additional 24 h at 37°C, after which the diameters of the zones of inhibition were measured.

2.5.2. Determination of MIC and MBC of PE-AgClNPs

The minimum inhibitory concentration (MIC) and minimum bactericidal concentration (MBC) of the PE-AgClNPs were determined by the twofold dilution method with minor modifications. (*29*)

2.5.3. Synergistic antibacterial potential of PE-AgClNPs

The synergistic effects of PE-AgClNPs with two antibiotics (kanamycin and rifampicin) were determined by the disc diffusion method, with slight modification (*30*). A total of 500 µL of PE-AgClNPs at 1000 µg/mL and 500 µL of each antibiotic at 200 µg/mL were mixed and sonicated for 15 min at room temperature, after which 50 µL of the mixture containing 25 µg/disc of PE-AgClNPs and 5 µg/disc of the standard antibiotics were impregnated into a filter paper disc and dried. Petri plates with NA media were spread with different pathogens and the nanoparticle/antibiotics discs were placed on it and incubated at 37°C for 24 h. The synergistic antibacterial activity was

measured by the diameter of zones of inhibition around the nanoparticle/antibiotics discs.

2.5.4. Synergistic anticandidal potential of PE-AgClNPs

The synergistic anticandidal potential of PE-AgClNPs with standard amphotericin b was determined against five pathogenic *Candida* species (*C. albicans* KACC 30003 and KACC 30062, *C. glabrata* KBNO6P00368, *C. geochares* KACC 30061 and *C. saitoana* KACC 41238) by the standard disc diffusion method (*31*). All the strains of *Candida* except *C. glabrata* KBNO6P00368 [obtained from the Chonbuk National University Hospital (Cheongju, Republic of Korea)] were obtained from the Korean Agricultural Culture Collection (KACC, Suwon, Republic of Korea). Prior to the test, both PE-AgClNPs at 2 mg/mL and amphotericin b at 200 µg/mL were mixed equally in a 1:1 ratio and sonicated for 15 min at room temperature. PE-AgClNPs/amphotericin b paper discs were prepared by adding 50 µL of the PE-AgClNPs/amphotericin b mixture on a paper disc containing 50 µg AgNPs and 5 µg amphotericin b/disc. The potato dextrose agar plates were spread uniformly with respective *Candida* strains and the AgNPs/amphotericin b paper discs were placed over them. The plates were incubated at 28°C for 48 h and the diameters of the zones of inhibition around each paper disc were measured to determine the synergistic anticandidal activity of the PE-AgClNPs/amphotericin b mixture solution.

2.6. Free radical scavenging and antioxidant potentials of PE-AgClNPs

The antioxidant potentials of the PE-AgClNPs were determined by DPPH free radical scavenging, ABTS free radical scavenging, nitric oxide scavenging and reducing power assay.

2.6.1. DPPH free radical scavenging assay

The DPPH free radical scavenging potential of PE-AgClNPs was determined according to a standard procedure (*32*). Briefly, 100 µL of the reaction mixture consisted of 50 µL of the PE-AgClNPs (20–100 µg/mL) and 50 µL of 0.1 mM DPPH in methanol. The control was composed of a reaction mixture of 50 µL of methanol and 50 µL 0.1 mM DPPH in methanol. The positive control was composed of a mixture of 50 µL of ascorbic acid (20–100 µg/mL) and 50 µL of 0.1 mM DPPH in methanol. The reaction mixture was mixed properly and incubated at 37°C with shaking at 150 rpm for 30 min in darkness. Following incubation, the absorbance was recorded at 517 nm using a microplate reader. The percentage scavenging effect of PE-AgClNPs was calculated from the following equation:

$$\%\text{DPPH radical scavenging} = \frac{\text{Abs}_c - \text{Abs}_t}{\text{Abs}_c} \times 100,$$

where Abs_c is the absorbance of the control and Abs_t is the absorbance of the treatment.

2.6.2. ABTS free radical scavenging assay

The ABTS radical scavenging activity of PE-AgClNPs was determined according to the standard procedure (*33*). Prior to the experiment, a stock solution of 7.4 mM ABTS and 2.6 mM potassium persulfate was prepared, mixed in equal volume and kept in darkness for 12 h to generate the ABTS working solution. After 12 h of incubation, the ABTS working solution was diluted appropriately with methanol to obtain an absorbance value of 1.1 ± 0.02 units at 750 nm. Next, 15 µL of PE-AgClNPs at different concentrations (20–100 µg/mL) was added to 135 µL of the ABTS reaction mixture and kept in darkness for 2 h. Fifteen microliter of methanol with 135 µL of ABTS reaction mixture was used as a negative control. The positive control was made by adding 15 µL of ascorbic acid at different concentrations (20–100 µg/mL) to 135 µL of the ABTS reaction mixture. Following incubation, the absorbance of the reaction mixture was recorded at 750 nm, and the percentage ABTS free radical scavenging activity was calculated according to the following equation:

$$\%\text{ABTS radical scavenging} = \frac{\text{Abs}_c - \text{Abs}_t}{\text{Abs}_c} \times 100,$$

where Abs_c is the absorbance of the control and Abs_t is the absorbance of the treatment.

2.6.3. Nitric oxide scavenging assay

The nitric oxide radical scavenging potential of PE-AgClNPs was determined by the standard method (*32*). Briefly, a 200 µL reaction mixture was prepared by mixing 100 µL of different concentrations of PE-AgClNPs (20–100 µg/mL) and 100 µL of 10 mM sodium nitroprusside in phosphate buffer saline (pH 7.4), then incubating the samples at 37°C for 1 h in light. A positive control was made by adding 100 µL of different concentrations of ascorbic acid (20–00 µg/mL) to 100 µL of 10 mM sodium nitroprusside in phosphate buffer saline (pH 7.4). After incubation, 75 µL aliquots of the reaction mixture were added to 75 µL of the Griess reagent (1.0% sulfanilamide and 0.1% naphthyl ethylene diamine dihydrochloride) in a 96-well flat bottom microplate (SPL Life Sciences, Gyeonggi-do, South Korea) and incubated at 25°C for 30 min in the dark. Following incubation, the absorbance was measured at 546 nm using a

microplate reader. A reaction mixture made of 100 µL of methanol and 100 µL of 10 mM sodium nitroprusside in phosphate buffer saline (pH 7.4) was taken as the negative control. The nitric oxide scavenging potential of PE-AgClNPs was calculated from the following equation:

$$\%\ \text{Nitric oxide scavenging} = \frac{\text{Abs}_c - \text{Abs}_t}{\text{Abs}_c} \times 100,$$

where Abs_c is the absorbance of the control and Abs_t is the absorbance of the treatment.

2.6.4. Reducing power assay

The reducing power of PE-AgClNPs was determined as previously described (*32*). The reaction mixture (150 µL) consisted of 50 µL of 0.2 M phosphate buffer (pH 6.6), 50 µL of 1% potassium ferricyanide and 50 µL of PE-AgClNPs at different concentrations (20–100 µg/mL). The reaction mixture was incubated at 50°C for 20 min in darkness. After incubation, the reaction was terminated by the addition of 50 µL of 10% trichloro acetic acid and centrifuged at 3000 rpm for 10 min. Next, 50 µL of supernatant was transferred to a 96-well microplate, amended with 50 µL of distilled water and 10 µL of 0.1% $FeCl_3$ solution, and further incubated for 10 min at room temperature. The absorbance of the solution was measured at 700 nm and the results were expressed in terms of the absorbance at 700 nm.

2.7. Statistical analysis

The results of all the experiments were expressed as the mean value of three independent replicates ± the standard deviation (SD). Significance differences between the mean values obtained among treatments were identified by one-way analysis of variance followed by Duncan's test at the 5% level of significance ($P < .05$) using the Statistical Analysis Software (SAS) (Version: SAS 9.4, SAS Institute Inc., Cary, NC).

3. Results and discussion

3.1. Synthesis and characterization of PE-AgClNPs

3.1.1. Synthesis of PE-AgClNPs

Biological methods for the synthesis of Ag nanoparticles are gaining importance in the field of nanoparticle synthesis. As a result of the growing success and simple processes for the formation of nanoparticles, the biological synthesis of Ag nanoparticles was attempted by reducing Ag^+ in $AgNO_3$ solution using the water extract of the peach outer peel (Figure 1, inset). The main cause of reduction of metal to metal nanoparticle is the presence of a number of enzymes and various types of phytochemicals such as flavonoids, phenolics, polysaccharides, terpenoids, etc. in the extracts of different plant and their parts (*6*,*34*). The preliminary confirmation of the reduction of metallic Ag to Ag nanoparticle was visually confirmed by a change in color of the reaction solution (Figure 1, inset) to reddish brown after 3 h of incubation. Because of the excitation of surface plasmon resonance, the color change in the reaction medium indicated the formation of Ag nanoparticles (*1*). Normally the gradual addition of the PE extract drop by drop to the reaction mixture resulted in the slow reduction of the $AgNO_3$ leading to the formation of small sized Ag^0 nanoparticles. Previous study have reported that the peach peel is rich in phenolics such as chlorogenic acid, catechins, epicatechins; and anthocyanins; flavonols along with a number of other compounds and amino acids (*19*,*24*–*26*), which were supposed to have been involved in the bio-reduction of metal substrate to AgClNPs.

3.2. Characterization of PE-AgClNPs

3.2.1. UV–Visible spectra analysis of PE-AgClNPs

In addition to the optical observation, the UV–Vis spectra of the reaction mixture were recorded at different time intervals from 0 min to 24 h. It is observed that the intensity of the peak increased with the increase in the incubation period with a maximum absorption peak at 440 nm at 24 h that ultimately confirmed the synthesis of Ag nanoparticles (Figure 1). The appearance of the brownish color of the synthesized PE-AgClNPs and the increase in the intensity of the peak was due to the excitation of the surface plasmon resonance, which is typical for AgNPs having λ_{max} values in the visible range of 400–500 nm (*35*). Similarly, several researchers have observed the absorption spectrum of Ag nanoparticles in between 425 and 460 nm due to the surface plasmon resonance of the AgNPs (*36*,*37*).

3.2.2. SEM and EDX analysis of PE-AgClNPs

The morphological characteristics of the synthesized PE-AgClNPs were observed under SEM (Figure 2(a) and (b)). The nanoparticles were agglomerated (Figure 2(a)), and the shape was somewhat spherical in nature (Figure 2(a)). The particle size distribution of the synthesized PE-AgClNPs ranged from 15 to 50 nm (Figure 2(b)). The average particle size of the PE-AgClNPs was found out to be 28.27 nm. The aggregation of the synthesized AgNPs might have been induced due to the evaporation of the solvent during the sample preparation and which also could have contributed to the variation in the particle size. Furthermore, the aggregation of the PE-AgClNPs might also have been possible due to the interactions such as hydrogen bond and electrostatic interactions

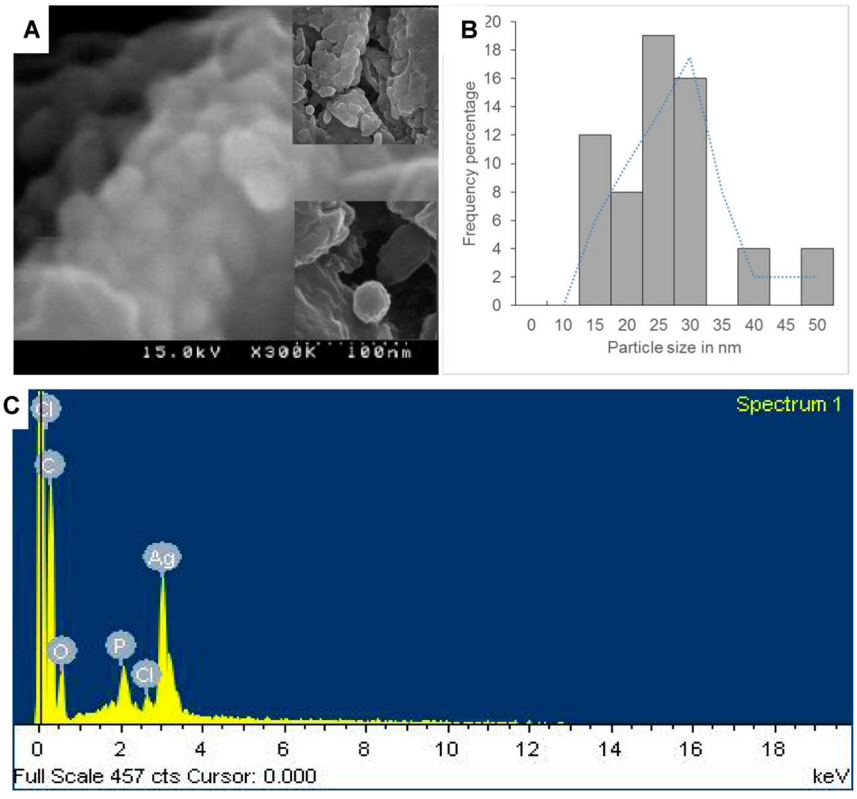

Figure 2. SEM image (a); size distribution graph (b) and EDX (c) of silver nanoparticles synthesized by the peach outer peel extracts.

between the bioorganic capping molecules that have bound to the PE-AgClNPs (*38*). Similar results were obtained previously using different plant extracts (*34*, *37*, *39*, *40*). EDX analysis confirmed the elemental composition of the synthesized nanoparticles (Figure 2(c)). The strong peak at 3 keV indicated the presence of the elemental Ag nanoparticles as evident from previous observations (*41*). Apart from Ag, other existing elements revealed by the EDX analysis included carbon, oxygen, phosphorous and chlorine which might be due to the X-

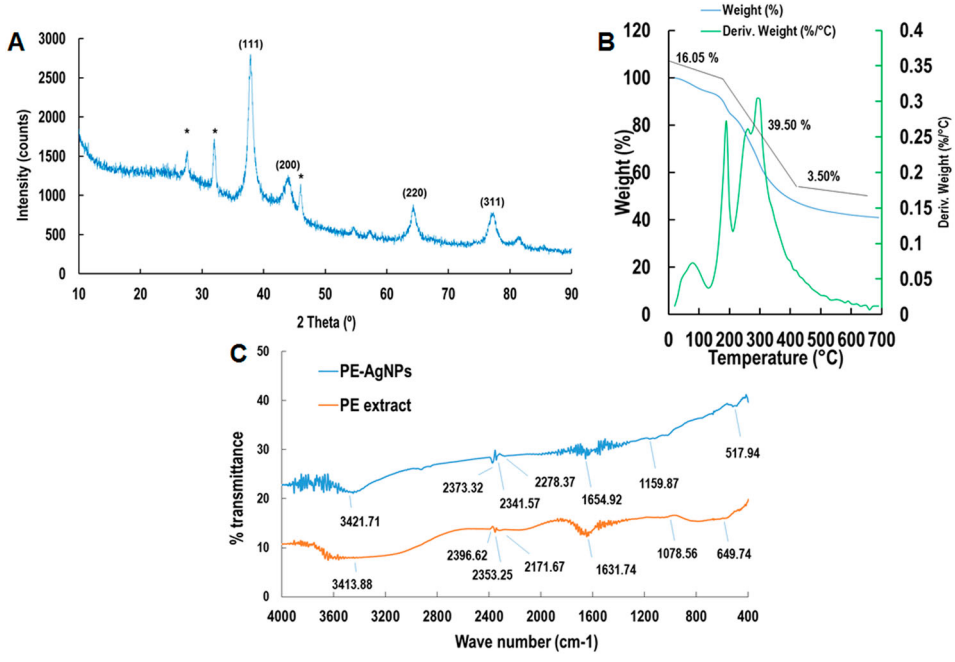

Figure 3. XRD (a), TGA (b; blue line is the TGA pattern of PE-AgClNPs and green line is the derivative weight of PE-AgClNPs) and FT-IR analysis (c) of silver nanoparticles (PE-AgClNPs) synthesized by the peach outer peel extracts (PE).

ray emission from the proteins/enzymes present in the PE extract. Since PE-AgClNPs were synthesized using the aqueous extract of peach outer peels, the presence of these elements confirmed that the organic metabolites present in the peel extract were responsible for capping and stabilization of the nascent nanoparticle (*42*).

3.2.3. XRD and TGA analysis of PE-AgClNPs

The XRD pattern of the synthesized PE-AgClNPs is shown in Figure 3(a). The diffraction pattern showed four well-resolved diffraction peaks (111, 200, 220, 311) corresponding to the standard FCC structures of Ag (JCPDS card no. 04–0783) (*43*). Apart from four distinct peaks, some unassigned peaks (*) were also observed in the XRD figure, which might have been due to crystallization of the bioactive components from the outer peel extract on the surface of PE-AgClNPs (*44*). These peaks are much weaker than those of the AgNPs that indicated that the Ag is the main material in the composite. These observation confirmed the crystallization of bioorganic materials on the surface of the synthesized silver nanoparticles. The results of TGA analysis of the synthesized PE-AgClNPs are shown in Figure 3(b). A total of 59.09% weight loss was observed in three different phases when the PE-AgClNPs were heated to 700°C. The first phase of weight loss was observed between 20°C and210°C with a weight loss of 16.05%. In this phase, the water molecules which were attached to the PE-AgClNPs were degraded. The second phase of weight loss was observed between 210°C and 490°C with a maximum weight loss of 39.50%. During this phase, the organic molecules from the PE extract which acted as capping and stabilizing agent for the synthesis of AgNPs were degraded. And the third phase extends from 500°C to 700°C with a weight loss of 3.50%. Gravimetric analysis of the PE-AgClNPs indicated the degradation of organic compounds from the PE extract that acted as capping agents for the PE-AgClNPs and their thermal stability at higher temperature (*45*).

3.2.4. FT-IR analysis of PE-AgClNPs

FT-IR analysis of the outer peel extract and PE-AgClNPs is shown in Figure 3(c). The absorption peaks located at 3413.88, 2396.62, 2353.25, 2171.67, 1631.74, 1078.56 and 649.74 cm^{-1} were shown by the outer peel extract, whereas the absorption peaks located at 3421.71, 2373.32, 2341.57, 2278.37, 1654.92, 1159.87 and 517.94 cm^{-1} were observed for the PE-AgClNPs (Figure 3(c)). The intense peaks located at 3421 and 3413 cm^{-1} corresponded to the O–H stretching of the alcohols and phenolic compounds, while the intense peaks at 1654 and 1631 cm^{-1} corresponded to–C=C–H stretching of alkenes group (*5*, *32*). The peak 1631 cm^{-1} in the PE extract has been shifted to 1654 cm^{-1} in the PE-AgClNPs. Similarly the peak at 1078 cm^{-1} and 649 cm^{-1} has also been shifted to 1159 cm^{-1} and 517 cm^{-1}, respectively in the PE-AgClNPs. The shifting in the position of different peaks in the PE-AgClNPs from the outer peel extract might have been due to progression of the reduction reaction with capping and stabilization of PE-AgClNPs by the various secondary metabolites present in the plant extract (*42*). The results showed that the synthesis of the PE-AgClNPs was possible due to the functional groups such as amines, alcohols, alkenes and phenolic groups present in PE extract (*46*).

3.2.5. Antimicrobial potential of PE-AgClNPs

The PE-AgClNPs were evaluated for their antibacterial potential against five different types of foodborne pathogenic bacteria; namely, *B. cereus* ATCC 13061, *E. coli* ATCC 43890, *L. monocytogenes* ATCC 19115, *S. aureus* ATCC 49444 and *S. Typhimurium* A TCC 43174 (Table 1). PE-AgClNPs at 50 µg/disc exhibited promising antibacterial activity against three foodborne pathogenic bacteria, *B. cereus* (9.03 mm inhibition zone), *E. coli* (10.83 mm inhibition zone) and *S. aureus* (9.01 mm inhibition zone); however, they did not show any activity against *L. monocytogenes* and *S. Typhimurium*. The MIC and MBC values of PE-AgClNPs against the bacteria were determined to be 50 µg/mL and 100 µg/mL, respectively (Table 1).

Resistance to different types of antibiotics by a number of foodborne pathogenic bacteria is one of the greatest challenges to public healthcare worldwide (*5*, *16*, *47*). Accordingly, there is a need to develop more potent antimicrobial drugs to overcome these problems. The broad spectrum antibacterial potential of PE-AgClNPs can be found in their usage in biomedical applications and

Table 1. Antibacterial activity of PE-AgClNPs (50 µg/disc) against five foodborne pathogenic bacteria.

Bacteria	PE-AgClNPs	$AgNO_3$	PE	DMSO	MIC (µg/mL)	MBC (µg/mL)
B. cereus ATCC 13061	9.03 ± 0.27^{b}*	0	0	0	50	100
E. coli ATCC 43890	10.83 ± 0.25^{a}	0	0	0	50	100
L. monocytogenes ATCC 19115	0^{c}	0	0	0	0	0
S. aureus ATCC 49444	9.01 ± 0.15^{b}	0	0	0	50	100
S. Typhimurium ATCC 43174	0^{c}	0	0	0	0	0

*Data are expressed as the mean zone of inhibition in mm ± SD. Values in the same column with different superscript letters are significantly different at $P < .05$.
$AgNO_3$ – 1 mM (10 µl/disc); PE extract (10 µL/disc), 5% DMSO (10 µL/disc).

treatment against various pathogens. When compared with other metals, Ag exhibits greater toxicity to microorganisms and lower toxicity to mammalian cells (*48, 49*). The synthesized PE-AgClNPs showed varied antibacterial activity against the tested foodborne pathogenic bacteria which might be due to the different morphological structure of the bacterial cell. It is assumed that, PE-AgClNPs might have destroyed the bacterial cell walls by rupturing the cell membrane either by penetration into the cell and impairing the respiration due to diminution of energy compounds or by cell membrane damage (*37 50*). It is supposed that due to smaller size in the nanoscale range, the PE-AgClNPs could have bound to the biomolecules of bacteria such as DNA or RNA and could have inhibited their uncoiling and transcription, resulting in the cellular toxicity leading to cell death (*51*). The efficiency of AgNPs against different types of bacteria varied due to the variable shape and size of the synthesized AgNPs using different plant sources and other biological systems (*52*). Antimicrobial activities of the PE-AgClNPs could also find applications in packaging of food items. These materials novelty in life, form a continuing antibacterial material with high temperature stability and low volatility (*5*). Foodborne bacteria can grow in packaging, leading to illness and diseases; therefore, packaging food with PE-AgClNPs can efficiently reduce bacterial growth in food containers (*53–55*).

PE-AgClNPs combined with kanamycin and rifampicin were evaluated for synergistic antibacterial potential against five foodborne pathogenic bacteria (Table 2, Figure 4(a) and (b)). PE-AgClNPs at 25 µg/disc, kanamycin at 5 µg/disc and rifampicin at 5 µg/disc did not contain any antibacterial activity, while PE-AgClNPs mixed with kanamycin or rifampicin at these concentrations exerted antibacterial activity. PE-AgClNPs combined with kanamycin actively controlled the growth of all five bacteria with inhibition zones ranging from 8.84 to 12.28 mm (Table 2). PE-AgClNPs combined with rifampicin was active against three foodborne bacteria, *B. cereus* (9.59 mm inhibition zone), *E. coli* (9.42 mm inhibition zone) and *S. aureus* (14.70 mm inhibition zone) (Table 2, Figure 4(B)). These data clearly demonstrated that antibacterial activity increased by mixing the prescribed antibiotics such as kanamycin or rifampicin with PE-AgClNPs. It is seen that at lower concentrations, the AgNPs are not effective, however when they were mixed with the standard antibiotics, their activity increased, the possible reason behind this activity might be due to the enhanced bacterial binding by AgNPs assisted by the standard antibiotics, kanamycin and rifampicin (*56*). A more probable cause of the synergistic effect may be the potential use of the AgNPs as the drug carrier. The bacterial cell membrane consists of phospholipids and glycoprotein, which are all hydrophobic in nature and thus they prevent the entry of the antibiotics into them, but the AgNPs due to their smaller size enters the target cells mixed with the antibiotics and kills the pathogen (*57, 58*). The results also matched with those of previous studies of the synergistic activity of AgNPs in combination with antibiotics (*58–60*). The current intensive use of antibiotics is leading to more rapid development of bacterial resistance; therefore, resistant strains are able to survive and even multiply in the presence of an antibiotic. Previous studies indicated improved controlling activity by adding compounds to the traditional antibiotics (*60*). Our study also demonstrated that PE-AgClNPs with conventional antibiotics exerted synergistic effects on foodborne bacteria, suggesting the possible use of lower concentrations of antibiotics to reduce mammalian cell toxicity and decrease pressure on bacteria to gain resistance.

The synergistic anticandidal effect of the PE-AgClNPs and amphotericin b was studied against five strains of pathogenic *Candida* species (Table 3 and Figure 4(c)). The results showed strong anticandidal synergistic activity against all the strains of *Candida* species (10.51–14.01 mm inhibition zones) with highest activity against *C. glochare* (14.01 mm inhibition zones). This synergistic anticandidal potential of PE-AgClNPs could make it a potential candidate for treatment against a number of *Candida* infections.

Table 2. Synergistic antibacterial activity of PE-AgClNPs (25 µg) with standard antibiotics, kanamycin (5 µg) or rifampicin (5 µg), against foodborne pathogenic bacteria.

Bacteria	PE-AgClNPs + Kanamycin	PE-AgClNPs + Rifampicin
B. cereus ATCC 13061	$11.60 \pm 0.17^{*b}$	9.59 ± 0.01^{b}
E. coli ATCC 43890	11.34 ± 0.67^{c}	9.42 ± 0.24^{b}
L. monocytogenes ATCC 19115	8.84 ± 0.19^{d}	0^{c}
S. aureus ATCC 49444	12.28 ± 0.25^{a}	14.70 ± 0.13^{a}
S. Typhimurium ATCC 43174	11.01 ± 0.18^{c}	0^{c}

*Data are expressed as the mean zone of inhibition in mm ± SD. Values in the same column with different superscript letters are significantly different at $P < .05$.

Table 3. Synergistic anticandidal activity of PE-AgClNPs (50 µg) with standard antifungal agent, amphotericin b (5 µg), against pathogenic *Candida* species.

Candida	PE-AgClNPs + amphotericin b
Candida albicans KACC 30003	$11.47 \pm 0.91^{bc*}$
Candida albicans KACC 30062	12.94 ± 0.12^{ab}
Candida glabrata KBNO6P00368	10.51 ± 0.23^{c}
Candida glochares KACC 30061	14.01 ± 0.11^{a}
Candida saitoana KACC 41238	11.28 ± 0.20^{bc}

*Data are expressed as the mean zone of inhibition in mm ± SD. Values with different superscript letters are significantly different at $P < .05$.

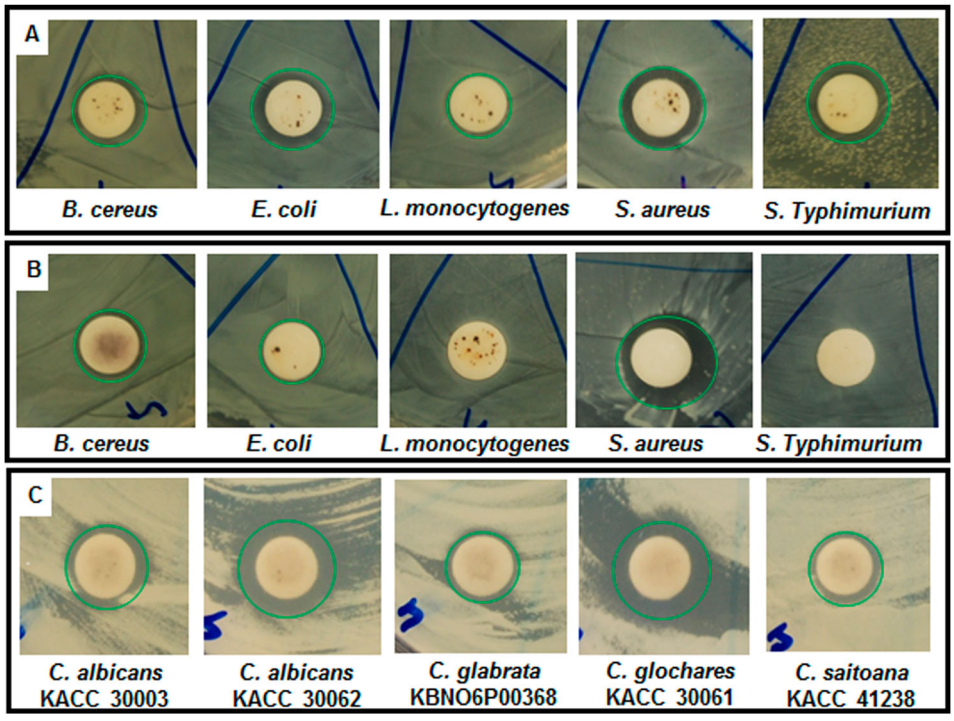

Figure 4. Synergistic antibacterial potential and anticandidal activity of silver nanoparticles synthesized by the peach outer peel extracts. The green circles represent the diameter of zone of inhibition.

3.2.6. Free radical scavenging and antioxidant potential of PE-AgClNPs

The free radical scavenging and antioxidant potential of PE-AgClNPs was evaluated by DPPH free radical scavenging, nitric oxide scavenging, ABTS radical scavenging and reducing power assay. PE-AgClNPs displayed concentration-dependent activity on DPPH free radical scavenging potential with 80.33% activity at 100 µg/mL (Figure 5(A)). Similarly, ascorbic acid (the reference compound) exerted 38.04% activity at 100 µg/mL (Figure 5(A)). PE-AgClNPs had higher DPPH free radical scavenging activity than ascorbic acid at all-tested concentrations (100 µg/mL). The effects of PE-AgClNPs on DPPH radical might have been due to their hydrogen donating activity (*61*).

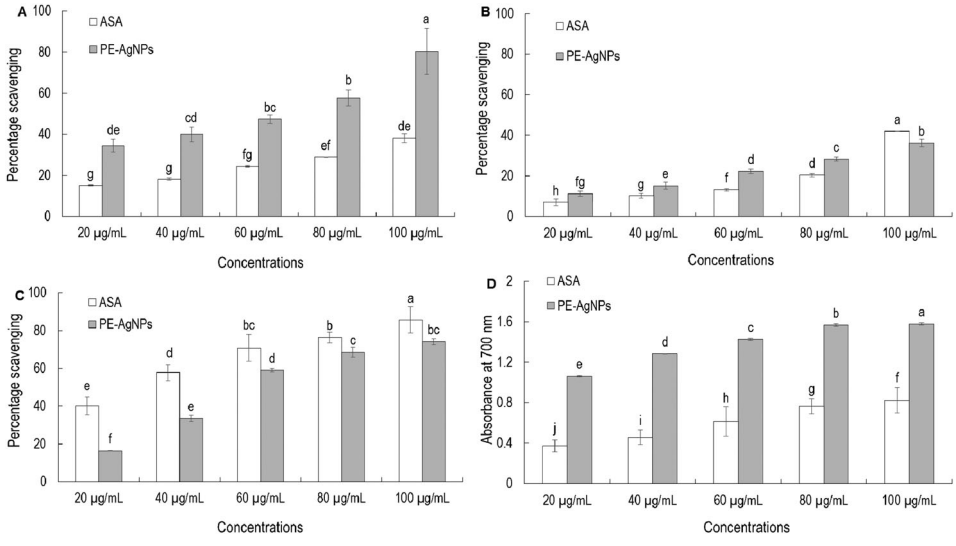

Figure 5. Antioxidant activity of silver nanoparticles synthesized by the peach outer peel extracts. DPPH free radical scavenging (A), nitric oxide scavenging (B), ABTS radical scavenging (C) and reducing power (D) potential of silver nanoparticles (PE-AgClNPs) and ascorbic acid as the reference compound. Different superscript letters in each column indicate significant differences at $P < .05$.

The nitric oxide scavenging potentials of PE-AgClNPs and ascorbic acid are presented in Figure 5(B). Both PE-AgClNPs and ascorbic acid displayed concentration-dependent activities over nitric oxide scavenging potential, with 36.18% and 41.92% scavenging at 100 µg/mL, respectively. Internally generated nitric oxides are very unstable and associated with various types of degenerative conditions including cancer, cardiovascular disease and inflammatory diseases (*62*). Therefore, the high nitric oxide scavenging of PE-AgClNPs could make them a potential candidate for application in biomedical sciences.

The ABTS radical scavenging potential and reducing power of PE-AgClNPs and ascorbic acid are presented in Figure 5(C) and (D). PE-AgClNPs and ascorbic acid displayed strong ABTS radical scavenging potential with 74.05% and 85.58% activity at 100 µg/mL, respectively (Figure 5(C)). When the reducing power of PE-AgClNPs and ascorbic acid were measured, PE-AgClNPs contained strong reducing power that was higher than the reference compound, ascorbic acid (Figure 5(D)). Strong reducing power of PE-AgClNPs represents its strong antioxidant potential, which might be due to the reducing agents contained in the peach outer peel.

The antioxidant potential of AgNPs synthesized using different plant extracts has previously been reported (*61*, *63–65*). All of the antioxidant activities tested using PE-AgClNPs revealed that PE-AgClNPs had strong antioxidant activities, which might be due to the secondary metabolites in the outer peel extracts such as phenolic compounds, anthocyanins and flavonols (*19*, *24–26*) that acted as capping and stabilizing agents for the AgNPs. The interaction of different types of phytochemicals present in the PE extract with the metal ions during the nanoparticle synthesis might have resulted into improved free radical scavenging compounds. Furthermore, the electrostatic attractions between the negatively charged secondary metabolites from the plant and the positively or neutrally charged AgNPs acted synergistically to improve the antioxidant potential of the PE-AgClNPs.

4. Conclusions

The present study demonstrated the utilization of outer peel extracts of peach for the synthesis of Ag nanoparticles, which is a positive step toward development of a cost-effective and environmentally friendly procedure for green nanoparticle synthesis using biological waste. The synthesized PE-AgClNPs had a surface plasmon resonance at 440 nm with an average particle size of 55.95 nm calculated from the XRD graph. PE-AgClNPs displayed potent antibacterial activity and synergistic activity with two conventional antibiotics, kanamycin and rifampicin, against foodborne pathogenic bacteria, as well as promising strong antioxidant potential. Overall, PE-AgClNPs possess prospective applications in the biomedical and food sector industries.

Disclosure statement

No potential conflict of interest was reported by the authors.

Funding information

This work was supported by grants from the Systems and Synthetic Agro-biotech Center through the Next-Generation BioGreen 21 Program (PJ011117), Rural Development Administration, Republic of Korea.

Notes on contributors

Jayanta Kumar Patra, working as assistant professor in Research Institute of Biotechnology & Medical Converged Science, Dongguk University, Ilsandong, Republic of Korea.

Kwang-Hyun Baek, working as Associate Professor in Department of Biotechnology, Yeungnam University, Gyeongsan, Republic of Korea.

References

(1) Chitra, K.; Annadurai, G. *J. Nanostr. Chem.* **2013**, *3*, 9. DOI: 10.1186/2193-8865-3-9
(2) Wijnhoven, S.W.P.; Peijnenburg, W.J.G.M.; Herberts, C.A.; Hagens, W.I.; Oomen, A.G.; Heugens, E.H.W.; Roszek, B.; Bisschops, J.; Gosens, I.; Meent, D.V.D.; Dekkers, S.; Jong, W.H.D.; Zijverden, M.V.; Sips, A.J.A.M.; Geertsma, R.E. *Nanotoxicology* **2009**, *3*, 109–138.
(3) Sondi, I.; Salopek-Sondi, B. *J. Colloid Interf. Sci.* **2004**, 275, 177–182.
(4) Krishnaraj, C.; Jagan, E.G.; Rajasekar, S.; Selvakumar, P.; Kalaichelvan, P.T.; Mohan, N. *Colloid. Surf. B* **2010**, 76, 50–56.
(5) Rajeshkumar, S.; Malarkodi, C. *Chem. Appl.,* **2014**, 2014, 1–10. DOI:10.1155/2014/581890
(6) Dipankar, C.; Murugan, S. *Colloid. Surf. B* **2012**, 98, 112–119.
(7) Babu, S.; Velez, A.; Wozniak, K.; Szydlowska, J.; Seal, S. *Chem. Phys. Lett.* **2007**, 442, 405–408.
(8) Mohanpuria, P.; Rana, N.K.; Yadav, S.K. *J. Nanoparticle. Res.* **2008**, *10*, 507–517.
(9) Farooqui, M.A.; Chauhan, P.S.; Krishnamoorthy, P.; Shaik, J. *Dig. J. Nanomater. Biostruct.* **2010**, *5*, 43–49.
(10) Ghodake, V.P.; Kininge, P.T.; Magdum, S.P.; Dive, A.S.; Pillai, M.M. *J. Eng. Res. Studies* **2011**, *2*, 32–36.
(11) Nithya, G.; Hema Shepangam, N.; Balaji, S. *Arch. Appl. Sci. Res.* **2011**, *3*, 377–380.
(12) Patra, J.K.; Baek, K.H. *J. Nanomater.* **2014**, *2014*, 1–12. DOI:10.1155/2014/417305

(13) Khalil, M.M.H.; Ismail, E.H.; El-Baghdady, K.Z.; Mohamed, D. *Arab. J. Chem.* **2014**, *7*, 1131–1139.
(14) Vimalanathan, A.B.; Tyagi, V.; Rajesh, A.; Devanand, P.; Tyagi, M.G. *World J. Pharm. Pharmaceutic. Sci.* **2013**, *2*, 2716–2725.
(15) Dauthal, P.; Mukhopadhyay, M. *J. Nanoparticle Res.* **2013**, *15*, 1366. DOI:10.1007/s11051-012-1366-7
(16) Ramamurthy, C.H.; Padma, M.; Daisy mariya samadanam, I.; Mareeswarana, R.; Suyavarana, A.; Suresh Kumarb, M.; Premkumarc, K.; Thirunavukkarasu, C. *Colloid. Surf. B* **2013**, 102, 808–815.
(17) Pizato, S.; Cortez-Vega, W.R.; De Souza, J.T.A.; Prentice-Hernandez, C.; Borges, C.D. *J. Food Safety* **2013**, *33*, 30–39.
(18) Scorza, R. *Peach and Apricot. Processing Fruits: Science and Technology*, 2nd ed.; CRC Press: New York, **2005**; pp 481–483.
(19) Zhao, X.; Zhang, W.; Yin, X.; Su, M.; Sun, C.; Li, X.; Chen, K. *Int. J. Mol. Sci.* **2015**, *16*, 5762–5778.
(20) Cheng, G.W.; Crisosto, C.H. *J. Amer. Soc. Hort. Sci.* **1995**, *120*, 835–838.
(21) Chang, S.; Tan, C.; Frankel, E.N.; Barrett, D.M. *J. Agric. Food Chem.* **2000**, *48*, 147–151.
(22) CevallosCasals, B.V.A.; Byrne, D.; Okie, W.R.; CisnerosZevallos, L. *Food Chem.* **2006**, *96*, 273–280.
(23) Infante, R.; Contador, L.; Rubio, P.; Aros, D.; PenaNeira, A. *Chil. J. Agri. Res.* **2011**, *71*, 445–451.
(24) Bakir, E.; Turker, N.; Istanbullu, O. *Gida.* **2007**, *32*, 15–23.
(25) Montevecchi, G.; Vasile Simone, G.; Mellano, M.G.; Masino, F.; Antonelli, A. *Fruits.* **2013**, *68*, 195–207.
(26) Iordnescua, O.A.; Alexaa, E.; Radulova, I.; Costeaa, A.; Dobreia, A.; Dobreia, A. *Agric. Agric. Sci. Procedia* **2015**, *6*, 145–150.
(27) Yousefzadi, M.; Rahimi, Z.; Ghafori, V. *Mater. Lett.* **2014**, *137*, 1–4.
(28) Diao, W.R.; Hu, Q.P.; Feng, S.S.; Li, W.Q.; Xu, J.G. *J. Agric. Food Chem.* **2013**, *61*, 6044–6049.
(29) Kubo, I.; Fujita, K.; Kubo, A.; Nihei, K.; Ogura, T. *J. Agric. Food. Chem.* **2004**, *52*, 3329–3332.
(30) Naqvi, S.Z.H.; Kiran, U.; Ali, M.I.; Jamal, A.; Hameed, A.; Ahmed, S.; Ali, N. *Int. J. Nanomed.* **2013**, *8*, 3187–3195.
(31) Murray, P.R.; Baron, E.J.; Pfaller, M.A.; Tenover, F.C.; Yolke, R.H. *Manual of Clinical Microbiology*, 6th ed.; ASM Press: Washington, DC, **1995**.
(32) Patra, J.K.; Baek, K.H. *Int. J. Nanomed.* **2015**, *10*, 7253–7264.
(33) Thaipong, K.; Boonprakoba, U.; Crosbyb, K.; Cisneros-Zevallosc, L.; Byrne, D.H. *J. Food Compos. Anal.* **2006**, *19*, 669–675.
(34) Bonde, S.R.; Rathod, D.P.; Ingle, A.P.; Ade, R.B.; Gade, A.K.; Rai, M.K. *Nanosci. Methods* **2012**, *1*, 25–36.
(35) Sadeghi, B.; Gholamhoseinpoor, F. *Spectrochim. Acta A.* **2015**, *134*, 310–315.
(36) Udayasoorian, C.; Kumar, K.V.; Jayabalakrishnan, R.M. *Dig. J. Nanomater. Biostruct.* **2011**, *6*, 279–283.
(37) Swamy, M.K.; Mohanty, S.K.; Jayanta, K.; Subbanarasiman, B. *Appl. Nanosci.* **2015**, *5*, 73–81.
(38) Priya, M.M.; Selvi, B.K.; John Paul, J.A. *Dig. J. Nanomater. Biostruct.* **2011**, *6*, 869–877.
(39) Tripathi, A.; Chandrasekaran, N.; Raichur, A.M.; Mukherjee, A. *J. Biomed. Nanotechnol.* **2009**, *5*, 93–98.
(40) Vivekanandhan, S.; Misra, M.; Mohanty, A.K. *J. Nanosci. Nanotechnol.* **2009**, *9*, 6828–6833.
(41) Kalimuthu, K.; Babu, R.S.; Venkataraman, D.; Bilal, M.; Gurunathan, S. *Colloids Surf. B.* **2008**, *65*, 150–153.
(42) Basavegowda, N.; Idhayadhulla, A.; Lee, Y.R. *Ind. Crop. Prod.* **2014**, *52*, 745–751.
(43) Khurana, C.; Vala, A.K.; Andhariya, N.; Pandey, O.P.; Chudasama, B. *Environ. Sci. Process. Impact.* **2014**, *16*, 2191–2198.
(44) Philip, D.; Unni, C.; Aromal, S.A.; Vidhu, V.K. *Spectrochim. Acta. Part A.* **2011**, 78, 899–904.
(45) Shaik, S.; Kummara, M.R.; Poluru, S.; Allu, C.; Gooty, J.M.; Kashayi, C.R.; Subbarao Subha, M.C. *Int. J. Carbohydr. Chem.* **2013**, *2013*, 10. DOI:10.1155/2013/539636
(46) Philip, D. *Spectrochim. Acta. Part A.* **2015**, *78*, 327–331.
(47) Boisselier, E.; Astruc, D. *Chem. Soc. Rev.* **2009**, *38*, 1759–1782.
(48) Wang, Y.; Cao, L.; Guan, S.; Shi, G.; Luo, Q.; Miao, L.; Thistlethwaite, I.; Huang, Z.; Xua, J.; Liu, J. *J. Mater. Chem.* **2012**, *22*, 2575–2581.
(49) Raja, S.; Ramesh, V.; Thivaharam, V. *Arab. J. Chem.* **2015**. DOI:10.1016/j.arabjc.2015.06.023.
(50) Ramesh, P.S.; Kokila, T.; Geetha, D. *Spectrochim. Acta. Part A.* **2015**, *142*, 339–343.
(51) Rai, A.; Prabhune, A.; Perry, C.C. *J. Mater. Chem.* **2010**, *20*, 6789–6798.
(52) Ashokkumar, S.; Ravi, S.; Kathiravan, V.; Velmurugan, S. *Spectrochim. Acta Part A.* **2015**, *134*, 34–39.
(53) Robertson, G.L. *Food Packaging: Principles and Practice*, 2nd ed.; CRC Press, Taylor & Francis: New York, **2006**.
(54) Rhim, J.W.; Ng, P.K.W. *Crit. Rev. Food Sci.* **2007**, *47*, 411–433.
(55) Finnigan, B. In *The Wiley Encyclopedia of Packaging Technology*; Yam, K.L., Ed.; John Wiley & Sons, New York, **2009**; pp 103–109.
(56) Mcshan, D.; Zhang, Y.; Deng, H.; Ray, P.C.; Yu, H. *J. Environ. Sci. Health C.* **2015**, *33*, 369–384.
(57) Ouay, B.L.; Stellacci, F. *Nano Today,* **2015**, *10*, 339–354.
(58) Li, P.; Li, J.; Wu, C.; Wu, Q.; Li, J. *Nanotechnology.* **2005**, *16*, 1912–1917.
(59) Ruden, S.; Hilpert, K.; Berditsch, M.; Wadhwani, P.; Ulrich, A.S. *Antimicrob. Agents Chemother.,* **2009**, *53*, 3538–3540.
(60) Hwang, I.; Hwang, J.H.; Choi, H.; Kim, K.J.; Lee, D.G. *J. Med. Microbiol.* **2012**, *61*, 1719–1726.
(61) Inbathamizh, L.; Ponnu, T.M.; Mary, E.J. *J. Pharm. Res.,* **2013**, *6*, 32–38.
(62) Cheng, R.; Glynn, S.; Santana, W.F.; Switzer, C.; Ridnour, L.; Wink, D.A. *Adv. Mol. Toxicol.* **2010**, *4*, 157–182.
(63) Mittal, A.K.; Kaler, A.; Banerjee, U.C. *Nano Biomed. Eng.* **2012**, *4*, 118–124.
(64) Abdel-Aziz, M.S.; Shaheen, M.S.; El-Nekeety, A.A.; Abdel-Wahhab, M.A. *J. Saudi Chem. Soc.* **2014**, *18*, 356–363.
(65) El-Rafie, H.M.; Hamed, M.A.A. *Adv. Nat. Sci: Nanosci. Nanotechnol.* **2014**, 5, 11. 035008. DOI:10.1088/2043-6262/5/3/035008